28 GHz Phased Array Interference Measurements and Modeling for a NOAA Microwave Radiometer in Manhattan

Abhishek Adhikari[1], Kevin Hermstein[1], Yonghua Wu[3], Thomas Legbandt[3], Carlos Caicedo Bastidas[2], Tingjun Chen[4], Fred Moshary[3], Ivan Seskar[5], Gil Zussman[1]

[1]Columbia University, [2]Syracuse University, [3]City College of New York, [4]Duke University, [5]Rutgers University

ABSTRACT

A microwave radiometer (MWR) at NOAA-CESSRST in Manhattan, NYC has experienced interference from nearby sources operating in the 5G FR2 n257 band (26.50–29.50 GHz). In this poster, we produce interference using a mobile 28 GHz IBM Phased Array Antenna Module (PAAM). The mobile PAAM leverages a software-defined radio which offers flexibility in varying center frequency, modulation, gain, bandwidth, time schedule, and more. In this poster, we show preliminary experiments which successfully created controlled interference to a MWR's 28 GHz channel which lead to distortion in some of the MWR final products, such as water vapor profile. We transmitted a 10 MHz bandwidth OFDM signal with varying amplitude, observing the highly sensitive MWR voltage response to fractional dB increments of the transmitter gain. The mobile PAAM is characterized in an anechoic chamber and MWR measurements are taken at various azimuth angles to help estimate the MWR antenna pattern. Future work will develop a Spectrum Consumption Model to help enable coexistence of MWRs and Beyond-5G networks.

CCS CONCEPTS

• **Networks → Wireless access networks**; • **Hardware → Wireless devices**.

KEYWORDS

mmWave, microwave radiometer, interference threshold

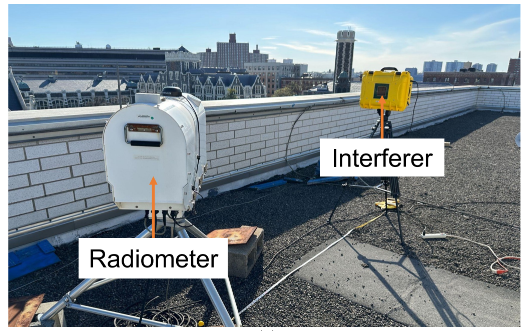

(a)

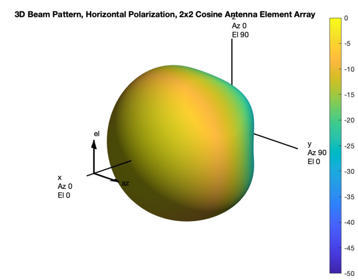

(b)

Figure 1: **(a) NOAA Radiometer and 28 GHz Phased Array Antenna Module (PAAM). (b) Simulated 28 GHz 2x2 phased array transmit beam representing configuration for generating interference with the PAAM.**

1 INTRODUCTION

5G and Beyond-5G wireless networks can leverage large amounts bandwidth available at mmWave bands to enable high data rate applications, but highly sensitive passive microwave radiometers (MWRs) rely on mmWave bands (specifically 20-30 GHz and 50-60 GHz) to sense vertical profiles of water vapor and temperature. These vertical profiles are eventually used for weather forecasting and climate modeling. As high data rate applications become more prominent (along with the needed mmWave infrastructure to go with it), there is a concern of these MWRs losing their ability to capture water vapor and temperature profiles due to radio frequency interference (RFI) nearby surpassing the sensitivity level of the instrument – essentially "drowning out" the subtle atmospheric attenuation fluctuation detected by the MWR. The International Telecommunication Union (ITU) has published documents about this known atmospheric attenuation [8].

NOAA Cooperative Science Center for Earth System Sciences and Remote Sensing Technologies (CESSRST) is located in Manhattan, NYC and hosts a MWR used by NOAA for weather forecasting [4]. NOAA CESSRST has already observed multiple instances of interference in the 28 GHz band when their MWR is pointed in the direction of George Washington Bridge (GWB) connecting New York City and New Jersey with mmWave deployments within a 200 meter radius. In this poster and illustrated in Figure 1(a), we intentionally interfere with the NOAA CESSRST MWR using a

ACM MobiCom '24, November 18–22, 2024, Washington D.C., DC, USA

ACM 979-8-4007-0489-5/24/11…
https://doi.org/10.1145/3636534.3697463

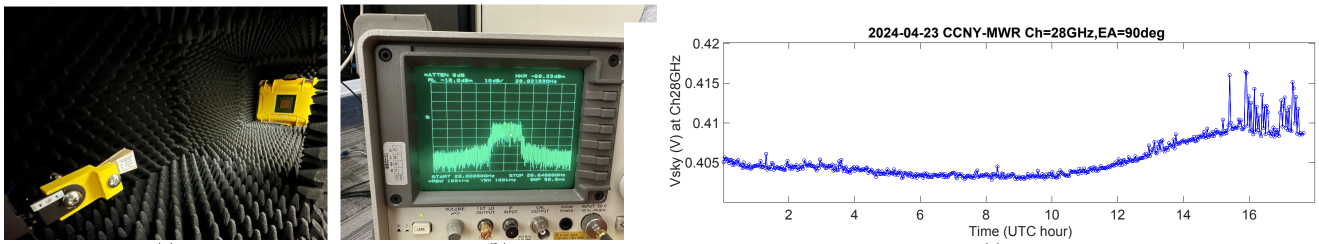

(a) (b) (c)

Figure 2: **(a) Verifying mobile PAAM functionality in an anechoic chamber with a spectrum analyzer. (b) Viewing the 10 MHz bandwidth OFDM signal transmitted by the PAAM 1 meter away on a spectrum analyzer. (c) MWR Level-0 data with interference beginning at 15:30 UTC.**

mobile 28 GHz IBM Phased Array Antenna Module (PAAM) traditionally used for mmWave communication research. We work with collaborators at NOAA CESSRST to determine if an acceptable level of interference can be determined for the eventual formulation of a Spectrum Consumption Model (SCM) to mitigate such interference using Dynamic Spectrum Access (DSA).

2 28 GHZ IBM RESEARCH PAAM

The PAAM contains 4 ICs, each with 16 elements. The up/down conversion takes place on the PAAM itself, and a 3 GHz IF can connect to a sub-6 GHz software defined radio (SDR) for a user to define waveform, center frequency, and transmit/receive (TX/RX) power [3, 6]. A mobile PAAM, consisting of a PAAM and SDR, was created to allow for mobile and outdoor experimentation with the PAAM [2]. Figure 1(b) shows a simulated beam pattern of what the PAAM transmitted in experiments shown in this research. The mobile PAAM leverages SDR to vary signal and radio parameters which helps in determining an interference threshold for the MWR. Intial calibration was performed in an anechoic chamber before outdoor experimentation, shown in Figure 2(a).

3 MWR WORKING PRINCIPLES AND DATA PROCESSING

The MWR operates with 35 different channels, each with a bandwidth of 300 MHz. Final products from the MWR include temperature, water vapor, and liquid water profiles at 58 different heights up to 10 km. These profiles, referred to as Level-2 data, are generated in a two-stage process. The first stage takes Level-0 voltage measurements and passes them through a transfer function to calculate the brightness temperature for each channel, known as Level-1 measurements. The 35 Level-1 values are then used as input features to the second stage, which is a pre-trained neural network (NN) model which generates the final Level-2 data.

Specifically, the Level-0 data consists of both measured values and calibrated parameters. Measurements occur over a full minute, allowing the radiometer to detect minute voltage changes necessary for weather sensing and reducing thermal noise, but also making it extremely sensitive to interference. The Level-1 data consists of the brightness temperature for each of the 35 channels. A brightness temperature is calculated from all Level-0 data of its corresponding channel according to:

$$T_{sky} = (V_{sky}/gain_{sky})^{(1/\alpha)} - T_{rcv-sky}, \quad (1)$$

where V_{sky} is the integrated received voltage from sky observation measured by the MWR; $gain_{sky}$ denotes the gain during sky observation derived from measured values and calibrated parameters; α is a nonlinearity correction exponent as a calibrated parameter; and $T_{rcv-sky}$ denotes the MWR receiver temperature during ambient black body target observation, which can be derived from measured values and calibrated parameters. Finally, the Level-2 data is generated by a NN, which is pre-trained using historical radiosonde soundings and a standard backward propagation method [7]. The input to the NN is the brightness temperature from all 35 channels and the output of the NN is the respective measurement at 58 different elevations up to 10 km, with higher granularity at lower elevations.

4 MWR INTERFERENCE USING PAAM

At the same rooftop as the MWR, we use the PAAM to transmit OFDM packets at a carrier frequency of 28 GHz with 10 MHz bandwidth, shown in Figure 2(b). Given the sensitivity of the MWR, we fine-tune the TX signal power at a resolution much more than built-in gain settings in GNU Radio, the signal processing platform commonly used with SDR [5]. The source signal is multiplied by a scaling factor of $\frac{1}{\sqrt{ScalingFactor}}$ to adjust the TX power levels. We measure the MWR Level-0 voltage while varying the scaling factor used for the PAAM. The Level-0 data is shown in Figure 2(c). Afterwards, we process the Level-0 data and determine when the Level-2 data becomes distorted. Figure 3 illustrates the full MWR processing pipeline from Level-0 to Level-2. We consult with NOAA CESSRST collaborators to identify at what point this distortion becomes a problem for their use cases of the data.

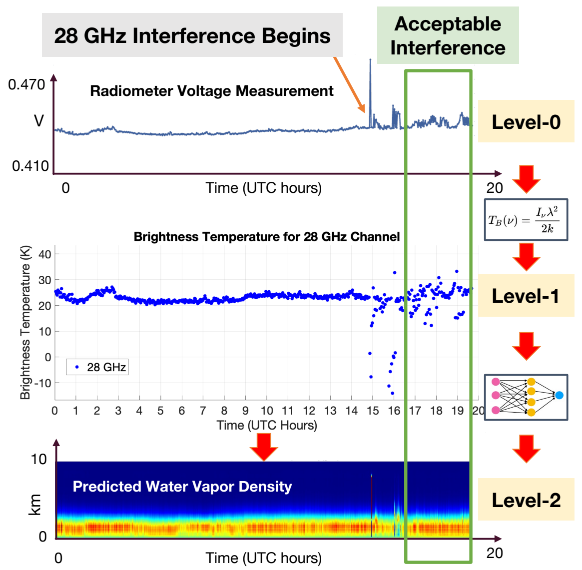

(a)

Figure 3: **Processing pipeline for MWR which uses Level-0 voltage to generate Level-1 brightness temperature and a Level-2 water vapor density profile.**

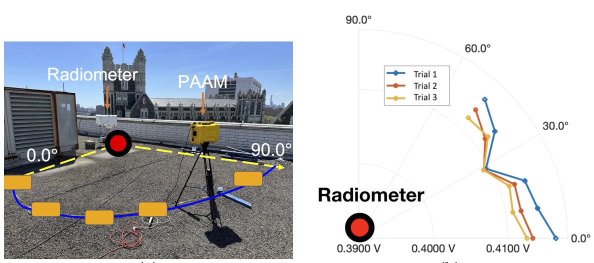

(a) (b)

Figure 4: **(a) Running several experiment trials to create interference at different azimuth angles ranging 0 to 60 degrees. (b) Estimating antenna pattern by viewing general interference threshold estimate at each azimuth angle.**

We also obtain an estimate of the MWR's 28 GHz channel receiver's antenna pattern. The challenge is the lack of physical space near the MWR to perform a full 360° sweep with the PAAM, and given sensitive wiring for the MWR, rotating the instrument itself would be too much of a risk. For these measurements, we estimate the antenna pattern for a 60° segment of the MWR by transmitting at a constant power from the PAAM and moving the PAAM along an arc centered around the MWR shown in Figure 4. These measurements in the field complement and enhance antenna pattern data from the MWR manufacturer.

5 CONCLUSIONS AND FUTURE WORK

We simulated interference observed by a MWR at NOAA-CESSRST to characterize the MWR's sensitivity to 10 MHz bandwidth OFDM interference at 28 GHz carrier frequency. We determined a threshold of allowable interference from the view of MWR Level-2 data. We computed such a threshold at various azimuth placements of the PAAM rotated between 0° and 90° centered around the MWR to estimate the MWR antenna pattern. However, this threshold should be similarly computed for the PAAM in scale of dBm in future work by characterizing the element-level gain and verifying linearity of the system. Also, given the MWR is outdoors with varying weather conditions, longer periods of data collection are necessary to generalize this threshold. Once such a threshold is determined and fully modeled, the next step will be in modeling interference and integration with spectrum sharing mechanisms, such as Spectrum Consumption Models standardized in IEEE 1900.5.2 [1].

6 ACKNOWLEDGEMENTS

This work was supported in part by NSF grants CNS-1827923, EEC-2133516, AST-2232455, AST-2232456, AST-2232458, AST-2232459, AST-2232460, CNS-2211944, and CNS-2128638.

REFERENCES

[1] Carlos E. Caicedo Bastidas, John A. Stine, Anthony Rennier, Matthew Sherman, Alex Lackpour, Mieczyslaw M. Kokar, and Reinhard Schrage. 2018. IEEE 1900.5.2: Standard Method for Modeling Spectrum Consumption: Introduction and Use Cases. *IEEE Comm. Standards Mag.* 2, 4 (2018), 49–55.

[2] Tingjun Chen, Prasanthi Maddala, Panagiotis Skrimponis, Jakub Kolodziejski, Xiaoxiong Gu, Arun Paidimarri, Sundeep Rangan, Gil Zussman, and Ivan Seskar. 2021. Programmable and Open-Access Millimeter-Wave Radios in the PAWR COSMOS Testbed. In *Proc. ACM WiNTECH'21.*

[3] Xiaoxiong Gu, Duixian Liu, Christian Baks, Ola Tageman, Bodhisatwa Sadhu, Joakim Hallin, Leonard Rexberg, Pritish Parida, Young Kwark, and Alberto Valdes-Garcia. 2019. Development, Implementation, and Characterization of a 64-Element Dual-Polarized Phased-Array Antenna Module for 28-GHz High-Speed Data Communications. *IEEE Trans. on Microwave Theory and Techniques* 67, 7 (2019), 2975–2984.

[4] The City College of New York. 2024. NOAA EPP Cooperative Science Center for Earth System Science and Remote Sensing Technologies Center. https://www.ccny.cuny.edu/noaa-cessrst

[5] GNU Radio. 2024. GNU Radio. https://www.gnuradio.org/

[6] Bodhisatwa Sadhu, Yahya Tousi, Joakim Hallin, Stefan Sahl, Scott K. Reynolds, Örjan Renström, Kristoffer Sjögren, Olov Haapalahti, Nadav Mazor, Bo Bokinge, Gustaf Weibull, Håkan Bengtsson, Anders Carlinger, Eric Westesson, Jan-Erik Thillberg, Leonard Rexberg, Mark Yeck, Xiaoxiong Gu, Mark Ferriss, Duixian Liu, Daniel Friedman, and Alberto Valdes-Garcia. 2017. A 28-GHz 32-Element TRX Phased-Array IC With Concurrent Dual-Polarized Operation and Orthogonal Phase and Gain Control for 5G Communications. *IEEE Journal of Solid-State Circuits* 52, 12 (2017), 3373–3391.

[7] Fredrick Solheim, John R. Godwin, E. R. Westwater, Yong Han, Stephen J. Keihm, Kenneth Marsh, and Randolph Ware. 1998. Radiometric profiling of temperature, water vapor and cloud liquid water using various inversion methods. *Radio Science* 33, 2 (1998), 393–404.

[8] International Telecommunication Union. 2012. Recommendation ITU-R P.676-9 - Attenuation by atmospheric gases. https://www.itu.int/dms_pubrec/itu-r/rec/p/R-REC-P.676-9-201202-S!!PDF-E.pdf